Influence of mask design on the growth of InGaAs/InAlAs quantum wells on patterned substrates

F. Racedo N., M. P. Pires, B. Yavich, L. C. D. Gonçalves and P. L. Souza

LabSem, Centro de Estudos em Telecomunicações,

Pontifícia Universidade Católica do Rio de Janeiro, Rua Marquês de São Vicente 225

Rio de Janeiro, 22453-900, Brazil

ABSTRACT

The influence of mask geometry on the growth enhancement and the alloy composition was investigated for InGaAs/InAlAs multiple quantum well structures grown on patterned InP (100) substrates by low pressure metalorganic vapor phase epitaxy. The masks used have a window 20 μm wide and width varying between 5 and 75 microns. Two different regimes have been observed. For masks with width smaller than 40 μm both growth enhancement and alloy composition influence the lowest optical transition energy, while for masks wider than 50 μm, alloy composition remains stable and the selectivity is essetially due to the growth enhancement. With the results obtained together with calculations of the Schrödinger equation within the effective mass approximation one concludes that, with proper mask design, it is possible to obtain an array of several modulators with slight different operation wavelength which are all polarization independent. In addition, the waveguiding characteristics of a modulator sample selectively grown was analysed by near field experiments. Comparing the results with a sample

conventionaly grown, one concludes that the selective growth technique essentially does not influence the waveguiding properties.

INTRODUCTION

The InGaAs/InAlAs multiple quantum well (MQW) system is of paramount importance for the development of amplitude modulators based on the quantum confined Stark effect (QCSE) for operation at 1.55 μm for telecommunication applications. The smaller valence band offset of the InGaAs/InAlAs structure, compared to InGaAs/InP, shortens the escape time of holes from the quantum wells making this material suitable for high intensity signal applications. Such structures have already given excellent performance characteristics as far as low operation applied voltage [1-3], large Stark shift [1,2], small chirp parameter [4] and polarization independence [2,3]. The monolithic integration of such a modulator with other devices is a promising way to both decrease its insertion losses and increase its operation frequency. Selective area growth (SAG) is the most promising technique for monolithic optoelectronic integration. This technique consists in growing layers on a patterned substrate and it is based on two effects, namely: enhancement of growth rate and modification of alloy composition. InGaAs/InAlAs MQW structures to be used in the fabrication of modulators to operate at 1.55 μm should have a precise lowest optical transition energy. This energy depends on both the growth enhancement and the alloy composition. The possibility of selectively growing InGaAs/InAlAs MQW structures by low-pressure metalorganic vapor phase epitaxy (LP-MOVPE) has already been demonstrated [5]. However, to controllably grow such structures by this technique, a better understanding of the growth enhancement and alloy composition as a function of the growth parameters and mask design is required.

The purpose of this work is to investigate both growth enhancement and alloy composition as a function of mask geometry for InGaAs/InAlAs MQW structures grown by selective area epitaxy on different patterned InP (100) substrates. These structures are specially designed to be used in the fabrication of amplitude modulators based on the QCSE. In addition, the influence of the SAG technique on the waveguiding properties were evaluated with near field and absorption experiments performed on a sample grown by SAG and on another one with an equivalent MQW structure, but grown on an unmasked substrate.

EXPERIMENTAL DETAILS

A horizontal low pressure, 100 mbar, MOVPE AIX 200 reactor was used for growing the samples. The total gas flow and temperature were 9800 sccm and 650ºC, respectively. The sources for the III elements were TMIn, TMGa and TMAl. AsH_3 was used as source for As with a mole fraction of 7.6×10^{-3} in all runs. The InP (100) oriented substrates were processed using specially designed masks with a fixed 20 μm wide window, which guarantees that selective area growth occurs in the gas phase diffusion regime [5]. The width of the masked region varied between 5 and 75 μm and its length was 1mm in the [100] direction. The masks were obtained by depositing 0.2 μm of silicon oxide.

InGaAs/InAlAs MQW structures were grown with input fluxes ratio [TMIn/(TMIn + TMGa(Al))] varying from 0.5 to 0.7. The different MQW structures had 15 or 20 periods, each unit had barriers 50 or 100 Å wide and quantum wells with thickness varying from 60 to 120 Å. The typical growth rate on unmasked substrates was about 1.5 to 2.0 Å/s.

The samples were characterized by spatially resolved photoluminescence (PL), x-ray diffraction and spatial profiler. A stylus profiler was used to determine the growth enhancement in the patterned regions. The 514 nm line of an Ar ion laser was used for excitation in the PL measurements. The laser beam was focused using a microscope objective lens of 25 mm focal length producing a beam diameter on the sample of 3 μm. The emitted signal was dispersed by a 250 mm monochromator and detected by a liquid nitrogen cooled Ge photodetector. The conventional lock-in technique was used for detection. Measurements were carried out at 77 and 300 K with an excitation power density of 40 KW/cm^2. X-ray experiments were performed on a double crystal diffractometer.

The modulator structures were investigated with near field measurements, where light from a 1.55 μm DFB laser is introduced in the waveguide with a single mode optical fiber with a microlens at the end for better coupling with the device. The light beam at the exit of the device is collected with a lenses system which magnifies the beam 75 times. The signal is then introduced into another single mode optical fiber which at its end is connected to an InGaAs photodetector. The photodetector is finally connected to the amplification system. The lock-in technique is used for detection. The detection optical system is mounted on x-y-z step motors with a step as small as 0.1 μm to allow a 2 dimensional scan of the guided beam. The third axis controls the focus.

RESULTS AND DISCUSSION

The growth enhancement for the MQW structures varied linearly for mask widths up to 75 μm for all the investigated samples, as determined from the stylus profiler measurements. An unpatterned substrate was always simultaneously introduced in the reactor to serve as a reference sample. The growth enhancement data were obtained with

respect to this reference sample. The total thickness of the samples on the unpatterned substrates varied from 0.2 to 0.4 μm. On the patterned substrates, the thickness measurements were always performed in the middle of the 20 μm window. It has been observed that the layer grown within the window was essentially flat starting at 2 microns from the mask borders. The growth enhancement (*GE*) as a function of mask width in microns (*W*) follows the expression given below for all samples. The deviation on the angular coefficient is smaller than 15%.

$$GE = 1 + 0.0150 \cdot W \qquad (1)$$

Figure 1 shows how the PL peak energy for several InGaAs/InAlAs MQW structures varies with mask width. One observes that an optical transition energy shift exceeding 200 meV with respect to the sample simultaneously grown on a reference unpatterned InP substrate was achieved for the wider mask and MQW structure with a 60 Å QW width and 50 Å barrier (sample 384). This result is comparable to the best values reported [5].

The width of the individual layers of the MQW structure in the window of the patterned regions can be evaluated by determining the width of the entire MQW structure with the stylus profiler and by taking into account the fact that the growth enhancement is essentially the same for both InGaAs and InAlAs [6]. Knowing the QW thickness and the lowest optical transition energy, it is possible to calculate the QW alloy composition by solving the Schrödinger equation within the one band effective mass approximation. The strain effects are included in the calculations. The results for two samples with different TMGa flows are plotted in figure 2, where one can see the variation of the Ga content in the

QW alloy as a function of mask width. The dotted lines are exponential fits which serve as a guide for the eyes. A clear saturation of the Ga content is observed for mask widths between 40 and 50 μm. Thus, two regimes can be distinguished. For masks with width smaller than 40 μm both growth enhancement and changes in alloy composition influence the optical transition energy, while for masks wider than 50 μm, the alloy composition remains stable and the selectivity is essentially due to the growth enhancement. With appropriate mask design, it should then be possible to have two integrated quantum well devices with the same alloy composition, lattice matched, for instance, and different optical transition energies. It should be noted that this effect is much more significant for the quantum wells than for the bulk samples [6].

In order to evaluate the influence of the SAG on the waveguiding and absorption properties along the plane of the layers, a modulator structure capable of guiding the light was grown, # 389. Sample 389 contains 20 periods of InGaAs/InAlAs quantum wells in between an InAlAs buffer layer of 0.3 μm, and an InAlAs cladding of 1.4 μm. The parameters for the MQW structure were chosen to give a lowest transition wavelength of 1.49 μm (appropriate for operation at 1.55 μm) and to have the heavy hole and light hole energies degenerate (polarization independence or $Ds = 0$) for a mask width of 45 μm. This width was chosen because for the growth rate used in our experiments, the sample quality was reproducibly better for the 45 μm wide mask line. Figure 3 shows the optical transition energy as a function of QW width where the solid squares are the experimental data for sample 389 for different mask widths. The position of the experimental points was determined using PL measurements at room temperature and the calibration of the growth rate on the patterned substrates (equation 1). The empty square represents a sample grown

on an unmasked substrate, sample 307, which is equivalent to the one selectively grown on the region of mask width equal to 45 μm. The dotted line is an exponential decay fit which serves as a guide for the eyes. The dashed line corresponds to the pairs [energy, well width] for which the heavy hole and light hole energies are degenerate. Each solid line corresponds to the lowest electron heavy-hole transition energy *vs.* QW width for a different Ga content in the quantum well alloy, *x*. The difference in *x* between two consecutive curves is 1%. These lines will be named $Dx = 0$ from now on. The solid and the dashed curves are obtained by solving the Schrödinger equation within the one band effective mass approximation. Strain effects are included. One can see from figure 3 that the experimental data points (dotted curve) show a decay which is more abrupt than both the $Ds = 0$ and $Dx = 0$ curves. For large mask widths, for which only the growth enhancement plays a role, as discussed above, one expects the experimental points to have the same steepness as the $Dx = 0$ curves. The lower limit for the steepness of the fit of the experimental data are, therefore, the $Dx = 0$ curves. So, it is possible to tailor the steepness of the experimental decay within a certain range by modifying the mask width. In particular, one can use a certain mask width range to force the abruptness of the experimental decay curve to be the same as that of the $Ds = 0$. Moreover, in order to make these curves coincide, one can change the growth conditions in such a way as to introduce an offset on the y-axis (different lowest electron heavy-hole transition energy for the structures grown on the unmasked region of the substrate). Hence, by properly choosing the growth parameters and the mask width, it is possible to obtain an experimental decay which coincides with the $Ds = 0$ curve. Thus, one can have on the same substrate several modulators operating at slight different wavelength, all polarization independent.

The inset shows a magnification of the central region of figure 3 where the solid line here corresponds to the experimental decay shifted along the energy axis so that it crosses the $D_s = 0$ curve at the empty circle. Experimentally speaking this corresponds to a slight change in the growth input parameters. As shown in the inset, for mask width varying between 40 and 50 μm, the maximum D_s obtained is 1.9 meV which already gives devices which are essentially polarization independent. This D_s is obtained for an operation wavelength range of 30 nm. For wavelength division multiplexing (WDM) applications, in such a wavelength range one fit 40 channels. If one uses a mask containing 40 parallel lines with 20 different widths varying between 40 and 50 μm (steps of 0.5 μm) and window of 20 μm, one can fabricate an array of 40 polarization independet modulators, each line width handling two channels. The two consecutive channels using the modulator structures grown on the same pattern present a variation in $\Delta\alpha$ (change in the absorption coeficiant between the on and off states) of only 3.4%, as estimated from fotocurrent measurment.

Figure 4 shows an atomic force microscopy picture of sample 389 after the 2.5 μm wide waveguide was processed on the 20 μm window which is surrounded by 45 μm wide mask lines. The picture demonstrates the good quality of the growth and photolithography. The near field image of the light after propagating along sample 389 is depicted in figure 5. The spot size of the beam in the growth direction is 1.7 μm and in the perpendicular direction is 2.8 μm. For such a spot size, the overlap of the optical mode with the active region of the modulator, G, reaches 0.077. The same experiment was performed with the reference, sample 307, and no deterioration of the signal due to the SAG technique was observed.

CONCLUSION

A detailed investigation of the selective area growth of InGaAs/InAlAs MQW structures for optoelectronic integration has been performed. For the growth conditions and mask geometries used in this work, a linear growth enhancement dependence on mask width was observed. In addition, a saturation of the alloy composition of the QW material in the MQW structures was observed for masks wider than 50 μm. This implies that for masks larger than this value, the alloy composition remains unchanged and growth enhancement dominates the SAG of InGaAs/InAlAs MQW.

It has been shown that, with the SAG under control and with proper mask design, an array of 20 different amplitude modulators all polarization independent, able to handle a 40 channels WDM system, can be fabricated.

Finally, near field experiments have demonstrated that the SAG technique does not affect the waveguide properties of the modulator.

ACKNOWLEDGEMENTS

The authors thank Alexandre Dal Forno for the help with the near field set-up and for many fruitful discussions. This work has been partially financed by Finep, CNPq and Faperj.

REFERENCES

[1] M. Pamplona Pires, B. Yavich, R. Pereira, P. L. Souza and W. Carvalho, 11th ICSMM, Hurghada, Egypt, July 1998.

[2] S. Chelles, R. Ferreira and P. Voisin, Applied Physics Letters **67**, 247 (1995).

[3] T. Ido, H. Sano, S. Tanaka, D. J. Moss and H. Inoue, J. of Lightwave Technology **14**, 2324 (1996).

[4] M. Pamplona Pires, B. Yavich and P. L. Souza, Applied Physics Letters **75**, 271 (1999).

[5] M. Tsuji, K. Makita, T. Takeuchi and K. Taguchi, Journal of Crystal Growth **170**, 669 (1997).

[6] B. Yavich, F. Racedo N., M. P. Pires, L. C. D. Gonçalves and P. L. Souza, Proceedings of the EW-MOVPE VIII – Prague 1999, p. 293 (1999).

FIGURES

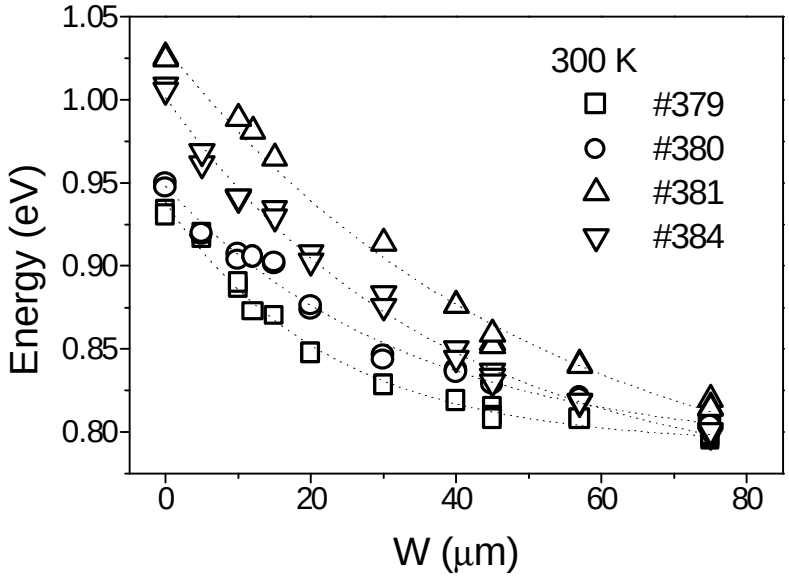

Figure 1: Lowest transition energy for a series of InGaAs/InAlAs MQW structures grown with various [TMIn/(TMIn + TMGa)] fraction in the gas phase and growth times as a function of mask width (*W*). The dotted lines are exponential decay fits.

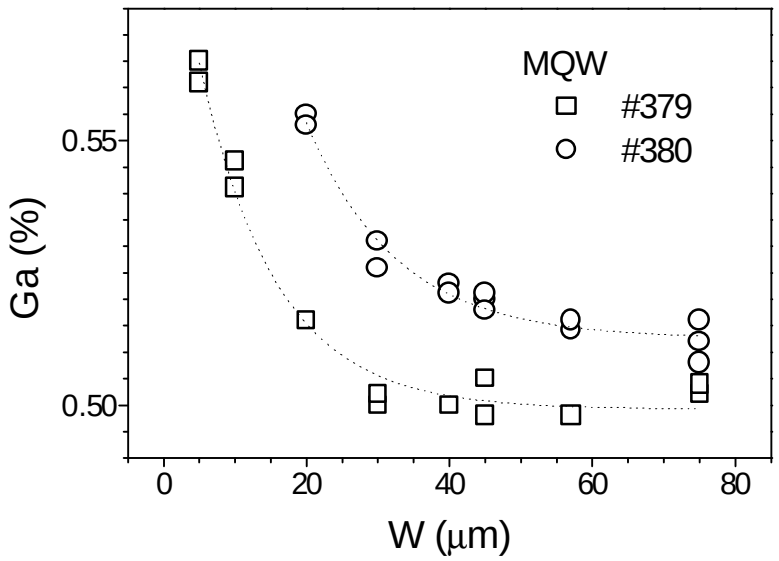

Figure 2: Ga content in the InGaAs QW alloy for two InGaAs/InAlAs MQW structures grown with different [TMIn/(TMIn + TMGa)] fraction in the gas phase as a function of mask width (*W*). The dotted lines are exponential decay fits.

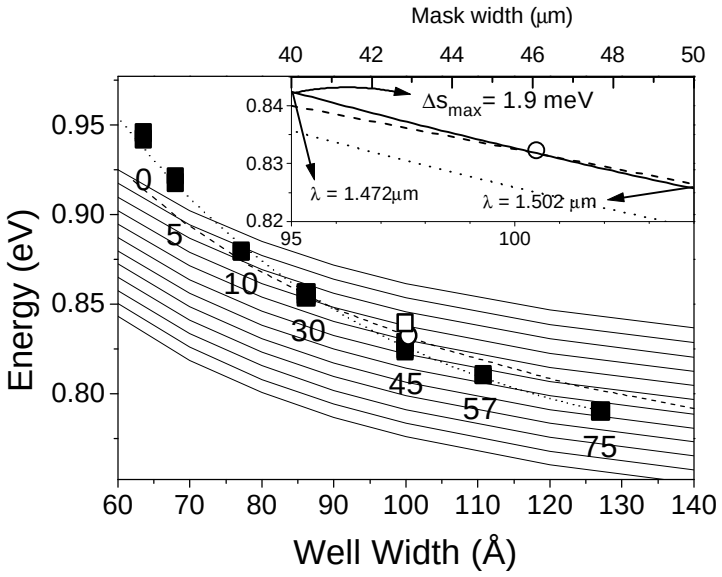

Figure 3: Optical transition energy as a function of QW width of an InGaAs/InAlAs waveguide structure grown on a patterned substrate containing mask lines of width varying from zero to 75 μm, sample 389. The solid squares are the experimental points for the different mask widths. The different widths are indicated in the figure. The dotted curve is an exponential fit of the experimental data. The empty square corresponds to the reference sample grown on an unmasked substrate, sample 307. Each solid line corresponds to the lowest electron heavy-hole transition energy *vs.* QW width for a different Ga content in the QW alloy, *x*. The difference in *x* between two consecutive curves is 1%. The dashed line represents the *Ds* = 0 curve. The empty circle is the intersection of the *Ds* = 0 curve and the transition energy 0.832 eV (1.49 μm) line. The inset is a magnification of the central region of the figure and its solid line is the experimental decay shifted upwards in energy.

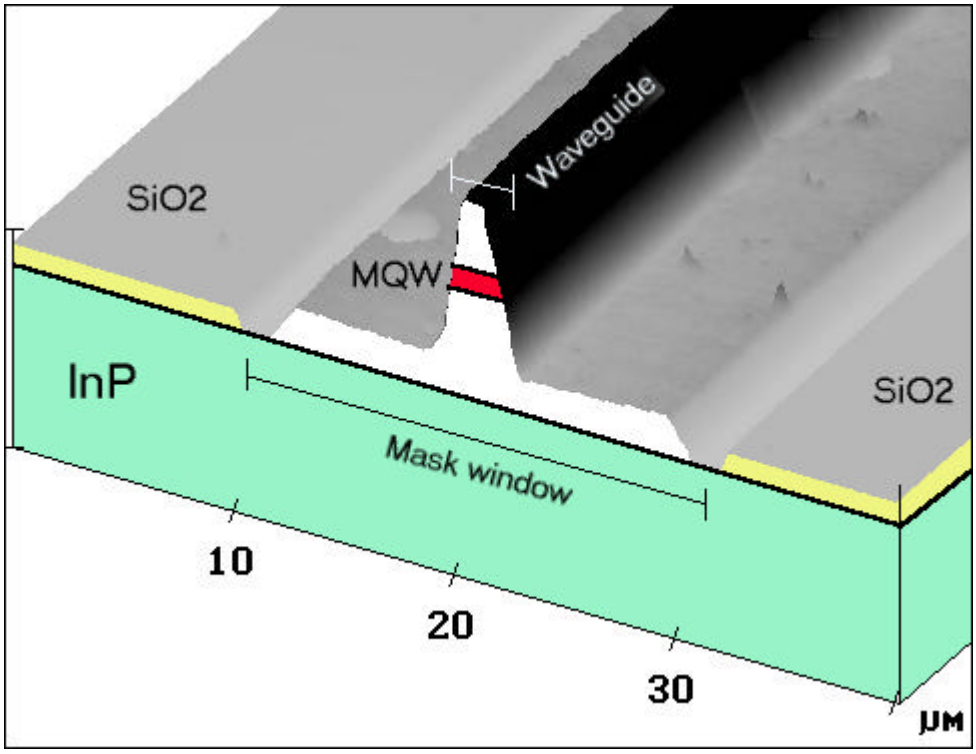

Figure 4: Atomic force microscopy picture of the waveguide sample grown on a patterned (100) InP substrate, sample 389. The waveguide was processed in the center of the 20 µm window which is surrounded by 45 µm wide mask lines.

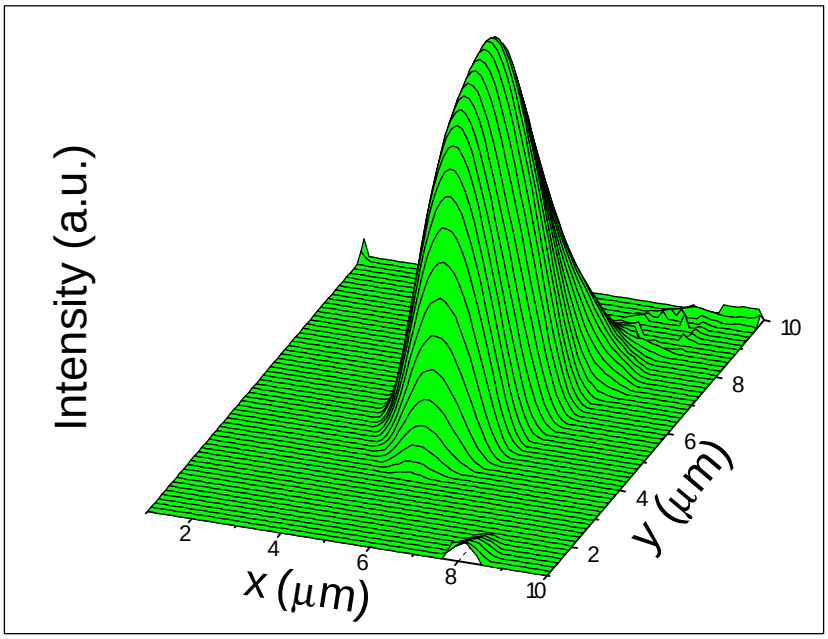

Figure 5: Near field image of the beam guided along the waveguide sample grown on a patterned (100) InP substrate, sample 389. The waveguide was processed in the center of the 20 μm window which is surrounded by 45 μm wide mask lines.